processes

MDPI

Article

Characteristics of Growth and Metabolism for Methane-Oxidizing Bacterial Communities in Different Coal Samples

Haojuan Ma [1,2], Ruilin Zhang [2,*], Yinbo Zhou [2], Kunyun Tian [2], Weidong Gong [2], Chaosheng Duan [1] and Shihai Chu [3]

[1] School of Safety Science and Engineering, Henan Polytechnic University, Jiaozuo 454003, China
[2] School of Resources and Safety Engineering, Henan University of Engineering, Zhengzhou 451191, China
[3] School of Energy Science and Engineering, Henan Polytechnic University, Jiaozuo 454000, China
* Correspondence: ruilinzhang@haue.edu.cn

Abstract

In recent years, microbial-mediated methane degradation, a technology represented by methane-oxidizing bacteria, has shown significant application potential in mine gas control. However, there are complicated interactions between underground coal bodies and microorganisms that can have a significant impact on bacterial community growth and metabolic activity. This study used bacterial fluids containing Xin'an (XA) and Yiluo (YL) coal samples as research subjects. The patterns of metabolic differential changes occurring during microbial growth under the effect of the coal matrix were discovered using an integrated application of gas–liquid-microbial-metabolism multi-omics analysis. The results showed that the addition of XA and YL coal samples did not significantly restrict the flora's methane oxidation efficiency, and instead, the addition of YL coal samples promoted the flora's methane degradation ability. The microbial community's amino acid metabolism went through a phased transformation, with proline and cysteine dominating at first and glutamic acid, aspartic acid, and serine accumulating subsequently, indicating adaptive metabolic adaptations under hypoxia. The nitrogen-containing and sulfur-containing compounds in the coal were degraded by the microbial communities, resulting in significantly higher SO_4^{2-} concentrations in the XA and YL groups compared to the CJY group, while NO_3^- concentrations decreased. Untargeted metabolomics analysis revealed that the addition of XA coal samples significantly affected the flora's nitrogen metabolism pathway, whereas YL coal samples significantly promoted the flora's sulfur metabolism, driving differential changes in metabolites such as aliphatic, peptide, purine nucleoside, benzene, heterocyclic, and organic acid metabolites as well as affecting the growth and metabolism characteristics of the microbial community and their activities. The research results have important theoretical and practical values for strengthening the theory of microbial methane degradation and enhancing the efficiency of methane-oxidizing bacteria in controlling coal mine gas.

Keywords: metabolic characteristics; methane-oxidizing bacterial community; coal; sulfur metabolism; nitrogen metabolism

check for updates

Academic Editor: Maria Jose Martin de Vidales

Received: 13 August 2025
Revised: 4 September 2025
Accepted: 6 September 2025
Published: 9 September 2025

Citation: Ma, H.; Zhang, R.; Zhou, Y.; Tian, K.; Gong, W.; Duan, C.; Chu, S. Characteristics of Growth and Metabolism for Methane-Oxidizing Bacterial Communities in Different Coal Samples. *Processes* **2025**, *13*, 2884. https://doi.org/10.3390/pr13092884

Copyright: © 2025 by the authors. Licensee MDPI, Basel, Switzerland. This article is an open access article distributed under the terms and conditions of the Creative Commons Attribution (CC BY) license (https://creativecommons.org/licenses/by/4.0/).

1. Introduction

As a companion product of coal, gas is mainly composed of methane. While methane is an efficient and clean energy source, its flammability and explosiveness pose a significant threat to subterranean safety in coal mines [1]. During coal mining operations, large

volumes of gas are released from coal seams into underground tunnels and working areas. Under certain conditions, this can result in major disasters such as coal and gas outbursts, gas combustion, and explosions as well as a variety of direct and indirect injuries, such as asphyxia and poisoning [2,3]. Furthermore, as the second most potent greenhouse gas, methane has a much higher GWP (Global Warming Potential) than carbon dioxide, accounting for 20% of worldwide greenhouse gas emissions, and coal mine emissions account for approximately 11% of total anthropogenic methane emissions [4,5]. Traditional coal mine gas management methods are mostly focused on managing the underground ventilation system [6] and enhancing gas extraction processes [7,8]. These measures can effectively reduce coalbed gas pressure and content, significantly suppressing the occurrence of gas accidents and mitigating their hazards. However, these methods require substantial investment of manpower and material resources. Furthermore, as coal mining size and depth rose in recent years, the permeability of coal seams decreased. A growing number of low-gas mines have become high-gas mines, while high-gas mines have evolved into coal and gas outburst mines. Coal mining and gas occurrence conditions are becoming increasingly complicated, making gas control more difficult [9]. Microbial-mediated methane degradation, represented by methane-oxidizing bacteria, is highly operable and requires low energy consumption, which is one of the effective ways of managing methane in an efficient and clean manner [10–12].

Methane-oxidizing bacteria are microorganisms that utilize methane as their sole carbon and energy source for growth and metabolism. They can be found in a variety of environments, including wetlands, landfills, rice paddies, and oceans [13–17]. Scientific researchers have studied methane-oxidizing bacteria extensively since the first strain, Bacillus methanicus, was identified and successfully isolated [18]. The growth mechanism of methane-oxidizing bacteria, the conditions under which methane degrades, improving the efficiency of bacterial methane oxidation, and the isolation and purification of degradation products are the four main areas of this study. Research on methane-oxidizing bacteria as functional microorganisms has gradually expanded into the engineering fields of environmental engineering and bio-energy and a variety of applications, including landfill methane abatement, oil and gas exploration, microbial fuel cells, and gas management in mines [1,19–21].

The concept of microbial control for coal mine gas was first proposed by coal chemist Jurowski. Since then, numerous researchers have focused their efforts on researching the applicability of this microbial technology in mine gas control [11,22,23]. Xie et al. [24] designed a microbial reactor using charcoal particles as packing material, which demonstrated outstanding degradation performance within a methane concentration range of 1–10%. Zhou et al. [25] analyzed the interaction potential between bacteria and coal from the perspective of methane-oxidizing bacteria's adsorption characteristics on coal and investigated the variation patterns of bacterial adhesion to different coal types. Han et al. [11] proposed mixing methane-oxidizing bacteria with a chelating wetting agent to effectively degrade methane, offering a novel approach for integrated reduction in rock burst susceptibility and gas pressure in deep coal mines. As studies progressed, academics found that the biodegradation process of methane in underground coal mine environments is influenced by dynamic interactions between microbial communities and the mineral components of the coal body. In mineral environments, microorganisms can degrade and modify minerals by secreting organic acids, siderophores, and redox to drive their weathering, dissolution, and precipitation [26–28]. David et al. [29] isolated four microbial strains from coal-containing sludge. After culturing these strains in coal-containing medium for 96 h, an analysis using UV spectroscopy at a wavelength of 450 nm demonstrated that these microbial strains have coal degradation capabilities. Ma et al. [30] proposed a gas desorption and permeability

enhancement technology based on native microorganisms in coal seams, which promoted the rapid decomposition of coal organic matter by optimizing the carbon–microorganism ratio. Liu et al. [31] used *Bacillus* sp. to degrade the harmful organic compounds in the coal gangue and found that the organic compounds in the gangue were gradually oxidized and activated under the action of microorganisms.

Similarly, minerals also exhibit specific regulatory effects on microbial activity. Xu et al. [32] studied the microbial communities and geochemical characteristics of five different functional zones in a coal mine and found a significant correlation between the distribution of microbial communities in the mine and the underground nutrient elements (e.g., C, S, P, and N) as well as redox-sensitive substances (e.g., Fe and As). Zhu et al. [33] discovered that the microbial community of acidified coal gangue has a strong nitrogen cycling function through rainfall simulation experiments. After the 15th day of the experiment, the abundance of microorganisms related to sulfur cycling increased, and the acidified coal gangue microorganisms exhibited stronger stress resistance than the newly formed community. Zhang et al. [34] investigated the impact of mining ultra-high organic sulfur Raša coal in Croatia on surrounding environmental microorganisms and found that high concentrations of PAH (polycyclic aromatic hydrocarbons) significantly reduced the diversity and abundance of microbial communities, revealing the shaping effect of coal-derived pollutants on microbial communities. Lian et al. [35] studied the changes in the composition of EPS (extracellular polymeric substances) under Cd(II) stress using Pseudomonas aeruginosa and Alcaligenes faecalis and discovered that adding $Cd(NO_3)_2$ significantly increased the protein content in these bacteria's EPS, thereby enhancing their heavy metal adsorption capacity. Furthermore, studies have demonstrated that mineral substrates can regulate microbial activity by influencing bacterial substrate utilization, respiratory metabolism, nitrification, and denitrification pathways [36–38].

Currently, the majority of the experimental studies on coal mine gas degradation using methane-oxidizing bacteria focus on the methane degradation efficiency of the bacteria at the coal scale, while the influence mechanism of coal sample characteristics on the metabolic function of the bacteria remains unclear. The complexity of the structure and composition of the coal samples means that the flora will show various dynamic responses and autoregulation characteristics to changes in environmental conditions. Therefore, this paper starts with the metabolic characteristics of the microbial community itself, using microbial solutions added to a Xin'an coal sample (XA) and Yiluo coal sample (YL) as research objects. Through the experiment of methane degradation by the microbial community, we tracked and tested the microbial community's ability to degrade methane, monitored the concentration changes of NO_3^- and SO_4^{2-} in the bacterial solution, and quantitatively analyzed amino acid changes during each stage of microbial community growth in combination with growth characteristics. In addition, untargeted metabolomics analysis of their metabolites using bioanalytical techniques was carried out to screen out intergroup signature differences in metabolites and major metabolic pathways in order to explore the molecular mechanism of the metabolic changes in the bacterial community affected by different coal sample environments. The results of this research can help to enrich basic theories on methane degradation by methane-oxidizing bacteria in coal mines and provide useful references for the development of new methods and technologies in the prevention and control of coal mine gas disasters.

2. Experimental Materials and Methods

2.1. Preparation of Coal Samples

The coal samples used in the experiments were selected from Henan Xin'an Coal Mine (XA) and Henan Yiluo Coal Mine (YL) (Table 1), which were crushed and sieved to obtain

samples with particle sizes ranging from 18 to 60 mesh. The samples were thoroughly washed with deionized water and dried for further use.

Table 1. Industrial analysis of coal samples.

Coal Sample	Industrial Analysis (%)			
	M_{ad}	A_d	V_{daf}	FC_{daf}
XA	1.21	5.53	36.87	55.06
YL	0.96	11.29	24.85	58.34

2.2. Cultivation of Microorganisms

Silt samples were collected from a 10 cm depth in the Shiqili River wetland in Xinzheng City, Henan Province, packed in a sterile bag, and brought back to the laboratory. A total of 5 g of silt sample was placed in a pre-sterilized and sterilized conical flask, 50 mL of sterilized ultrapure water was added and filtered after shaking well, and the supernatant was collected after 24 h of rest for the enrichment culture of the bacterial community.

(1) A total of 5 mL of supernatant was taken and injected into a threaded reagent bottle containing 50 mL of culture medium. NMS medium was used in the experiment [1], which was mixed with purified water. The composition and concentration of the culture medium are shown in Table 2. The culture medium and culture device were sterilized in an autoclave at 121 °C for 21 min.

(2) Reagent bottles were rinsed with high-purity methane, sealed, and placed in a constant temperature shaker for shaking culture (30 °C, 120 r/min). They were washed with high-purity methane every 24 h.

(3) After 5 days of cultivation, when the culture medium became turbid, 5 mL of the bacterial solution was transferred to 50 mL of fresh medium, and high-purity methane was used for gas rinsing again. The mixture continued to grow in the same environment.

(4) Steps 2 and 3 were repeated 10 times in a row to increase the purity of the methane-oxidizing mixed bacterial community. The process is depicted in Figure 1.

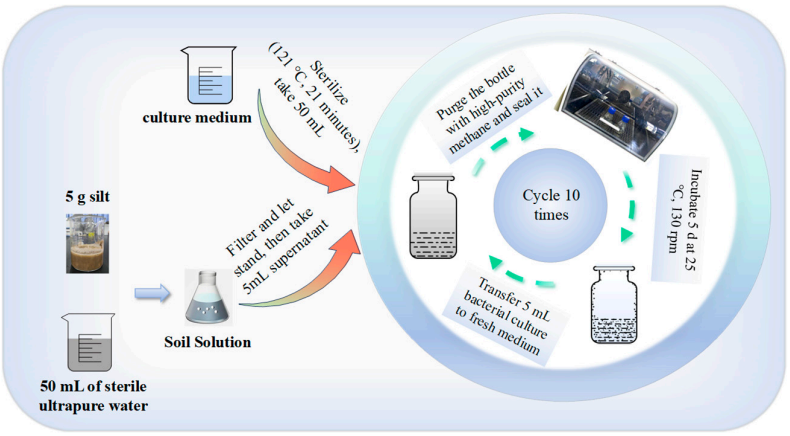


Figure 1. Flow chart of microbial community enrichment culture.

Microbial 16S rRNA sequencing was performed on the cultivated methane-oxidizing bacteria. The diversity and richness indices of the mixed microbial community are shown in Table 3. This sequencing yielded a total of 81,649 sequences, and 221 OTUs (operational taxonomic units) were obtained through sample clustering, with a sample coverage rate of 100%. For the index analysis, the Shannon index is used to measure community diversity, with higher values indicating higher diversity; the Simpson index also reflects diversity, but the higher the value, the lower the diversity. The Chao index and Ace index are commonly

used to estimate the total number of species or OTU abundance. The Shannon index characterizes the evenness of individual distribution of species in a community.

Table 2. NMS medium components.

Massive Element Solution		Trace Element Solution	
Reagents	**Ratios/(g·L^{-1})**	**Reagents**	**Ratios/(g·L^{-1})**
KNO_3	1.000	$CuSO_4 \cdot 5H_2O$	0.030
$MgSO_4 \cdot 7H_2O$	1.000	$FeSO_4 \cdot 7H_2O$	0.200
$Na_2HPO_4 \cdot 12H_2O$	0.717	$MnSO_4 \cdot 4H_2O$	0.003
KH_2PO_4	0.272	$ZnSO_4 \cdot 7H_2O$	0.010
NH_4Cl	0.250	Na_2EDTA	0.500
$CaCl_2 \cdot 6H_2O$	0.200	$NaMoO_4 \cdot 2H_2O$	0.003
		$NiCl \cdot 2H_2O$	0.002
Massive element solution: Trace element solution = 1000:1 (the volume ratio)			

Table 3. Analysis of diversity and richness index of methane-oxidizing bacteria mixed communities.

Sample	Number	OTUs	Shannon	Chao	Ace	Simpson	Shannoneven
original solution	81,649.00	221.00	1.64	227.16	237.59	0.35	0.30

The relative abundance of microbial communities at the species level is shown in Figure 2. At the genus level, these include Methylocystis (55.33%), Pseudoxanthomonas (15.22%), Terrimonas (11.98%), Acidovorax (8.41%), Hyphomicrobium (1.19%), unclassified Rhizobiaceae (1.33%), and Other (6.55%). Data indicates that the cultivated microbial community is a mixed consortium dominated by methane-oxidizing bacteria.

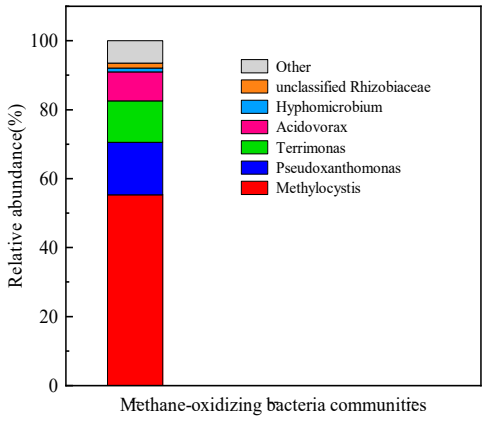


Figure 2. Composition structure of methanotrophic communities.

2.3. Analytical Testing Methods

2.3.1. Methane Degradation Test by Microbial Communities

The experiment utilized the pressure stabilization and gas retention experimental device designed by Zhou et al. [1]. In the specific experimental process, two groups of 100 mL of bacterial culture solution were taken, and 10 g of Xin'an (XA) coal samples and 10 g of Yiluo (YL) coal samples were added as the experimental groups, respectively. At the same time, a pure bacterial solution without a coal sample was set as the control group (CJY). The experimental devices of each group were rinsed with high-purity methane, sealed, and placed in a 30 °C incubator for cultivation. Every 24 h, 1 mL of the gas was extracted, and the concentration changes of CH_4, O_2 and CO_2 were detected using an Agilent 7890B gas chromatograph (Agilent Technologies Inc., Santa Clara, CA, USA) to

monitor the volume changes in each component gas. Each set of experiments involved three sampling and testing procedures, and the average value was calculated as the final experimental result.

2.3.2. Liquid Phase Inorganic Ion Concentration Test

A Thermo Fisher ICS-600 ion chromatograph (Thermo Fisher Scientific Inc., Waltham, MA, USA) was used to determine the concentrations of NO_3^- and SO_4^{2-} inorganic ions in the bacterial solution. The ion chromatography column was Dionex Ionpac AG22, and the ion chromatography guard column was Dionex Ionpac AS22 (Thermo Fisher Scientific Inc.). The column temperature was 30 °C. The suppressor current was 75 mA, and the flow cell temperature was 35 °C. The mobile phase was a mixture of Na_2CO_3 and $NaHCO_3$, with isocratic elution and a flow rate of 1.0 mL/min. A total of 0.5 mL of bacterial solution was transferred into a 5 mL volumetric flask, purified water was added to the mark, and the solution was mixed thoroughly. Then, the solution was slowly pushed into the 0.22 um membrane filter and RP ion chromatography pretreatment column in sequence, discarding the first 4.5 mL and retaining the remaining liquid for machine testing. Additional details on quality control and method performance can be found in Zhang et al. [39].

2.3.3. Amino Acid Test

A total of 0.5 mL of bacterial solution was added to a hydrolysis tube, and then, an equal volume of analytical pure hydrochloric acid was added. After nitrogen purging for 30 s, the tube was sealed and placed in an oil bath at 110 °C for 24 h of hydrolysis. After cooling to room temperature, the hydrolysate was filtered through a 0.45 μm membrane into a 50 mL volumetric flask and diluted to the mark. A total of 2 mL of the finished sample was transferred to a rotary evaporator for deacidification until a small amount of solid or trace stains remained at the bottom of the vial. A total of 2 mL of sodium citrate buffer was added to completely dissolve it, and then, it was filtered once more before being tested in an amino acid analyzer (Biochrom Ltd., Cambridge, UK). The buffer flow rate was set at 20 mL/hr, and the reaction flow rate was set at 10 mL/hr. The separation column was a Na-type cationic resin chromatography column. The ultraviolet detection wavelengths were 570 nm and 440 nm; the column temperature was 55–65–77 °C, programmed to increase, and the reaction bath temperature was 138 °C.

2.3.4. Untargeted Metabolomics Test

A total of 10 mL of the solution was placed in a freeze-dryer oven and lyophilized for 24 h (−20 °C, U-Al mode). After lyophilization, 100 μL aliquots were mixed with 400 μL of cold methanol acetonitrile solution (volume ratio of 1:1) and then allowed to stand for 30 min at −20 °C. The mixture was centrifuged for 20 min (14,000× g, 4 °C), and the supernatant was dried in a vacuum drying oven. The samples were centrifuged again for 15 min after being redissolved in 100 μL of acetonitrile water (volume ratio of 1:1) solvent for LC–MS analysis. The supernatant was taken for untargeted LC–MS detection and bioinformatic analysis. An Agilent 1290 Infinity LC UHPLC (Agilent Technologies Inc., Santa Clara, CA, USA) coupled to an AB Sciex TripleTOF 6600 quadrupole time-of-flight instrument (Sciex, Framingham, MA, USA) was used for the analysis, and three parallel groups were set up for each sample. In addition, 15 uL of supernatant was pipetted from each sample and mixed as QC (quality control) samples, respectively, which were used to examine the stability of the whole detection process.

The raw data were visualized and analyzed, and the extracted data were further subjected to metabolite structure identification and data preprocessing. The reliability of the results was examined using PCA (principal components analysis) and OPLS-DA (orthogonal partial least squares discriminant analysis). To screen for distinct metabolites

between groups, we set VIP (variable importance in projection) ≥ 1, FC (fold change) ≥ 1, and p (p-value) < 0.05. Then, KEGG (Kyoto Encyclopedia of Genes and Genomes) metabolic pathway analysis was performed on the different metabolites.

3. Experimental Results and Analysis

3.1. Effect of Different Coal Samples on the Methane Degradation Performance of Bacterial Colonies

The daily variations in CH_4, O_2, and CO_2 volumes during the CJY group's experiment are depicted in Figure 3a. According to the data, the total gas volume decreased by 139 mL in 15 days as the incubation period was extended. Of this, O_2 consumed 25.17 mL, CH_4 consumed 83.16 mL with a degradation rate of 92.8%, and CO_2 increased from 0.67 mL to 4.45 mL. The total gas volume decreased by 127.3 mL throughout the incubation time, according to the XA group's experimental data (Figure 3b). Of this, O_2 consumed 25.44 mL with a 100% volume decrease, CH_4 consumed 66.83 mL with a 79.33% volume decrease, and CO_2 increased from 0.66 mL to 3.87 mL. Within 15 days, group YL's total gas decreased by 125.5 mL (Figure 3c). Of this, O_2 consumed 24.51 mL, resulting in a 100% volume decrease, and CH_4 consumed 75.22 mL, with an effective degradation rate of 85.2%. The amount of CO_2 increased from 0.64 mL to 4.21 mL.

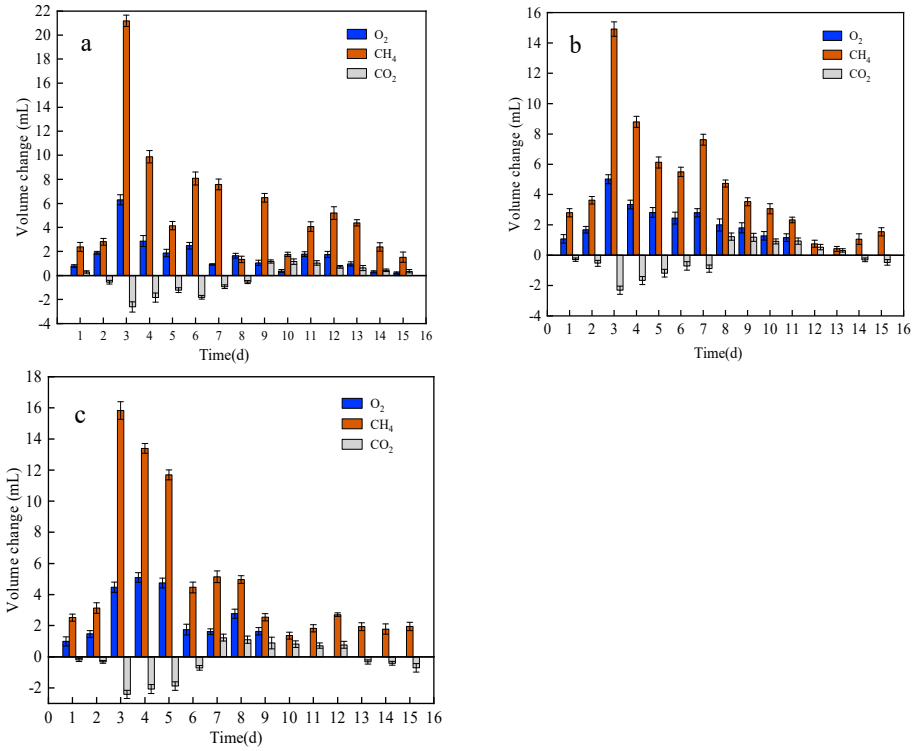


Figure 3. Daily volume changes in the three gases in three groups of experiments. (**a**) CJY group; (**b**) XA group; (**c**) YL group. Positive values represent consumption, and negative values represent generation.

During the entire experiment, the three experimental groups consumed near 25 mL of O_2, and the methane degradation rate was highest in the CJY group, followed by the YL group, and lowest in the XA group under similar O_2 conditions. This is because the aerobic microorganisms in the coal increased the consumption of O_2. The O_2 in groups XA and YL was depleted on the 11th and 9th days, respectively, and the methane-oxidizing community lacked sufficient O_2 to maintain the methane oxidation process, severely restricting the bacterial community's methane-oxidation capacity. Within 1 to 9 days of cultivation, the total amount of CH_4 consumed by the three experimental systems, CJY, XA, and

YL, was 63.84 mL, 57.64 mL, and 63.66 mL, respectively, with a small overall difference, especially in the YL group, which consumed almost the same amount as the CJY group. The experimental results showed that the addition of XA and YL coal samples did not significantly inhibit the methane degradation ability of the methane-oxidizing bacteria; on the contrary, the addition of YL coal samples helped to improve the methane-oxidizing efficiency of the bacteria under the condition of abundant oxygen, which showed a more excellent promotion effect.

It is worth noting that there was still a continuous consumption of methane in the XA and YL groups after the O_2 was depleted, but the methane-oxidizing ability of the communities weakened dramatically compared with that in the early stage of growth. This is because the microbial community chosen through experimentation was a mixed community dominated by methane-oxidizing bacteria and included a variety of aerobic and anaerobic bacterial genera. Among them, aerobic methane-oxidizing bacteria catalyze methane oxidation through MMO (methane monooxygenase), which relies on oxygen to convert methane into methanol [40]. Within 1 to 5 days of cultivation, the experimental system had enough oxygen to support the microbial community's methane degradation process. The microbial community was dominated by aerobic ethane-oxidizing bacteria, exhibiting strong methane degradation capabilities. The depletion of O_2 in the system lowered the activity of aerobic microbial communities, resulting in a significant decrease in CH_4 degradation efficiency compared to previous phases. Anaerobic methanotrophs eventually took over as the main population. This self-regulation function also reflects the advantages of microbial communities in gas disaster control, which can adapt to the complex environment to meet the needs of engineering practice.

3.2. The Changes in Liquid-Phase Inorganic Ion Concentration

As can be seen in Figure 4a, NO_3^- concentration showed a general trend of increasing and then decreasing. The NO_3^- concentration in the CJY group peaked on the fourth day, going from 571.90 mg/L to 702.70 mg/L, showing the greatest rise. The XA and YL groups peaked on the third day. The XA group grew from 579.17 mg/L to 622.76 mg/L, representing the second largest change. The YL group had the smallest rise, rising from 604.85 mg/L to 629.45 mg/L. At the beginning of cultivation, the environment was rich in nutrients, the bacterial community made extensive use of the nitrogen source as an energy source to promote its own growth, the amount of nitrate reduction was less than its production, and the NO_3^- concentration showed a rising trend. The NO_3^- concentrations in the three groups of experiments decreased significantly as the incubation time increased, showing that the microbial communities extensively utilized NO_3^- as a nitrogen source or electron acceptor for metabolic activities. Among them, the YL group showed the most significant decrease, from 628.44 mg/L on day 5 to 420.71 mg/L on day 16, indicating a greater nitrate utilization ability. Analyzing the reason for this, it is clear that, with the continuous depletion of O_2 in the culture environment, the activity of aerobic bacterial groups weakened, and anaerobic methane-oxidizing bacteria such as nitrate and nitrite gradually took the lead, and NO_3^- utilization continued to improve.

Figure 4b shows that, during the whole incubation period, the overall change in SO_4^{2-} concentration in the CJY group was relatively small. Within 1 to 4 days of cultivation, the SO_4^{2-} concentration in the XA and YL groups increased rapidly and nearly linearly compared to the CJY group, which fluctuated steadily. The SO_4^{2-} concentration in the XA group rose from 282.69 mg/L to 401.58 mg/L, a 39.53% rise, while the YL group's concentration increased from 280.25 mg/L to 371.30 mg/L, a 30.27% increase. It effectively indicates that the easily degradable sulfur-containing compounds in the XA and YL coal samples, especially in the XA coal sample, were oxidized to sulfate by the synergistic action

of microbial communities and thus degraded and released. When cultured on the 4th–7th day, the concentration of SO_4^{2-} in the three groups tended to stabilize, indicating that microbial communities' sulfate metabolism was stable in the absence of significant exogenous sulfur input. After entering the late stage (days 12–16), both the XA and YL groups showed a small increase in SO_4^{2-} concentration. The SO_4^{2-} concentration peaked at 447.94 mg/L in the XA group and 465.67 mg/L in the YL group. This phenomenon may be related to the oxidative release of refractory sulfur compounds in coal, particularly organic sulfur. Organic sulfur in coal samples primarily exists in the forms of thiophenes, mercaptans, carbonyl sulfide, sulfoxides, and sulfones. These molecules are embedded within the coal's carbon matrix in complex chelated forms, exhibiting structural stability and making the breakdown of organic sulfur in coal more difficult [41,42]. As the cultivation time increased, certain microbes may have gradually oxidized such organic sulfur compounds. The oxidation of sulfur-containing compounds exceeded the reduction of sulfates, increasing the concentration of SO_4^{2-} in solution. It is worth noting that the SO_4^{2-} concentration in the YL group gradually increased beginning on the 8th day of cultivation, indicating that the YL coal samples might contain more difficult-to-degrade sulfur-containing compounds or improved efficiency of microbial-mediated sulfur metabolism.

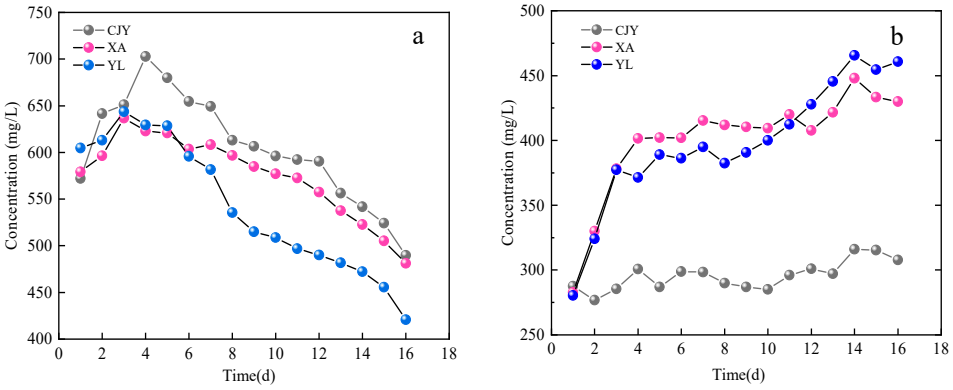


Figure 4. Variation in NO_3^- and SO_4^{2-} concentration in three groups of experiments. (**a**) The concentration of NO_3^-; (**b**) the concentration of SO_4^{2-}.

3.3. Changes in Dominant Amino Acids in Microbial Solutions

Figure 5 shows the comparison and analysis of the changes in the relative content of the top five dominant amino acids in the microbial solutions of the three experimental groups (CJY, XA, and YL) at the 4th, 8th, and 12th days of incubation. Pro (proline) dominated all three groups of microbial solutions during the early stages of incubation (day 4). Among them, the CJY group had the highest percentage of Pro at 22.77%, which can promote cellular osmoregulation, and the microbial communities maintain cellular homeostasis by accumulating Pro high osmotic pressure environments [43], indicating that the microbial communities are actively growing. In addition to Pro, Cys (cystine) also constituted a significant proportion of the microbial solutions in the CJY, XA, and YL groups, with percentages of 14.18%, 16.37%, and 14.29%, respectively. As a sulfur-containing amino acid, Cys can somewhat characterize the metabolic level of microbial sulfur-containing compounds [44]. The large proportion of Cys in the XA group indicates that more inorganic sulfur in the XA coal samples was oxidized by microorganisms to enter into the Cys synthesis pathway.

The relative contents of Glu (glutamate) and Asp (aspartate) in all groups increased significantly when the incubation time was extended. The results on day 8 showed that the CJY group had the highest total Glu and Asp content (21.59%), which was significantly higher than that of the XA (19.12%) and YL (18.95%) groups, and this trend remained

stable on day 12. As the core intermediates of nitrogen metabolism, the increase in the relative content of Glu and Asp indicates microbial nitrogen metabolism pathways are operating efficiently [45], providing effective support for bacterial growth. It is worth noting that the YL group had a considerable rise in the relative content of Ser (serine) at day 8 compared to day 4, and the same trend was observed in the XA group at day 12. Analyzing the reasons for this, it is clear that the depletion of O_2 and other nutrients in the culture environment restricted microflora growth. During the degradation of methane by methane-oxidizing bacteria, CH_4 is first oxidized to methanol by MMO, and methanol is further oxidized to formaldehyde by MDH (methanol dehydrogenase) [46]. Formaldehyde is a core intermediate metabolite in the metabolism of methane-oxidizing bacteria, and a decrease in methane oxidation efficiency in microbial communities may lead to the accumulation of formaldehyde. Formaldehyde is successively formed into formate and tetrahydrofolate by the action of some specific functional enzymes and finally converted into methylenetetrahydrofolate, which reacts with Gly (Glycine) to promote the synthesis of Ser [47,48].

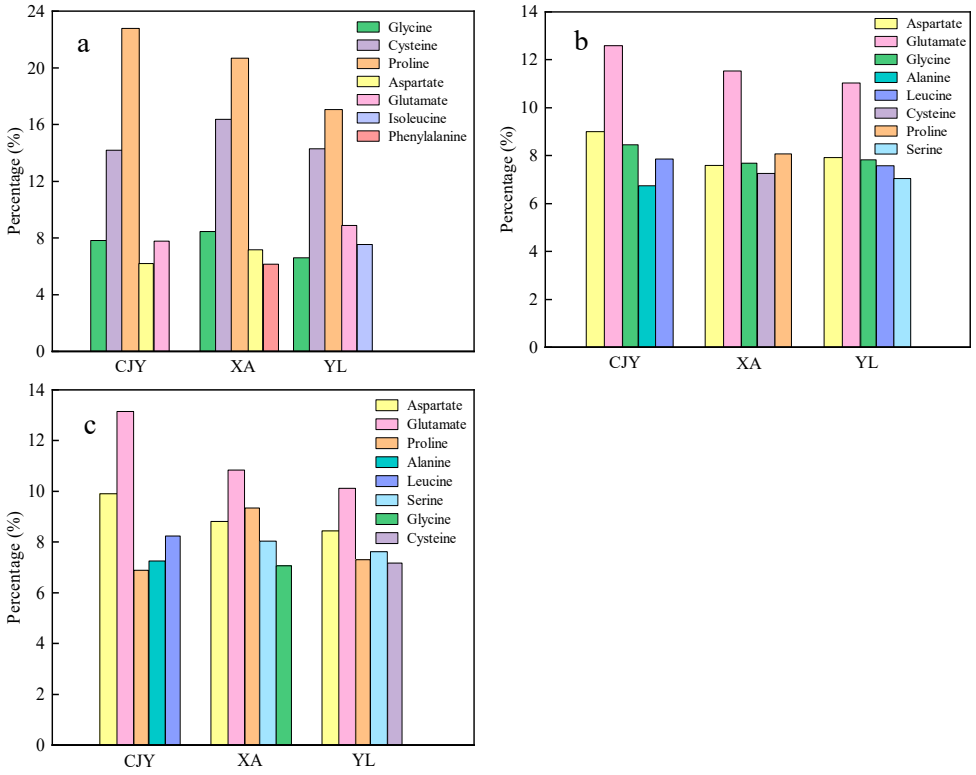


Figure 5. Changes in the percentage of dominant amino acids in the three groups of experiments. (**a**) Day 4 of cultivation; (**b**) day 8 of cultivation; (**c**) day 12 of cultivation.

3.4. Identification and Analysis of Differential Metabolites in Microbial Communities

3.4.1. Multivariate Statistical Analysis

The three groups of experimental metabolites were analyzed by untargeted metabolomics, and the results of PCA (Figure 6) showed that the CJY, XA, and YL groups were obviously separated in POS (positive) and NEG (negative) modes, indicating differences in their metabolites. Meanwhile, the QC samples were densely distributed, meaning that the data were reliable and that parallel samples repeated well. Among these, the positive and negative ion modes refer to the different voltage polarities used by the mass spectrometer during ESI (electrospray ionization). This process causes metabolites to form either positively or negatively charged ions for detection. Positive ion mode refers to the tendency of metabolite molecules (M) to acquire a proton (H^+) to form $[M+H]^+$ or to combine with a positive charge to generate

positively charged ions (e.g., $[M+Na]^+$). The negative ion mode refers to the tendency of metabolite molecules (M) to lose a proton (H^+) to form $[M-H]^-$ or bind to a negatively charged group to form a negatively charged ion (e.g., $[M+Cl]^-$).

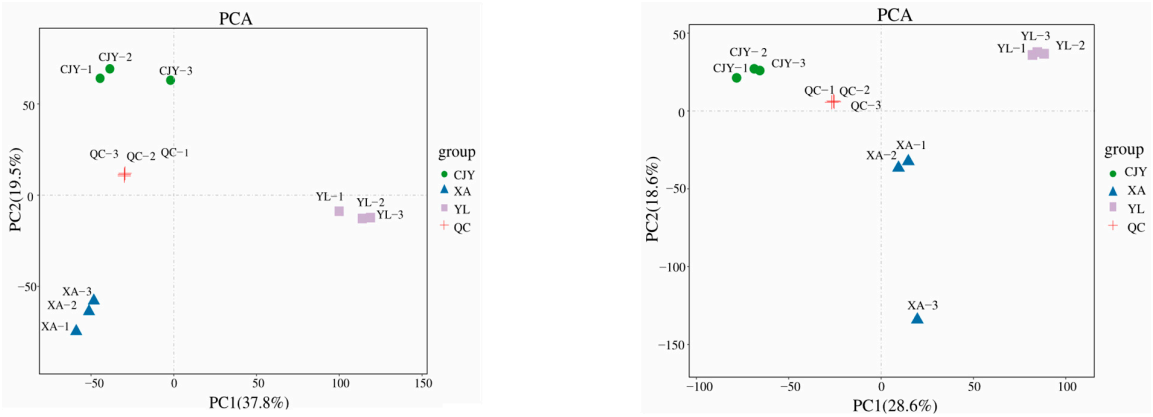


Figure 6. PCA score plots of POS and NEG ion modes for three groups of metabolites.

In order to more deeply analyze the sample distribution and obtain information about the differences between groups, the three groups of data were subjected to OPLS-DA. The results (Figure 7) showed a clear separation between CJY and XA as well as between CJY and YL, showing statistically significant differences between groups. The OPLS-DA model's validation parameters (Table 4) showed that R^2Y and Q^2 were near to 1 in both comparison groups, indicating that the model had strong explanatory and predictive power (R^2X and R^2Y represent the rate of explanation of the established model for the X-matrix and Y-matrix, respectively, and Q^2 represents the predictive power of the model).

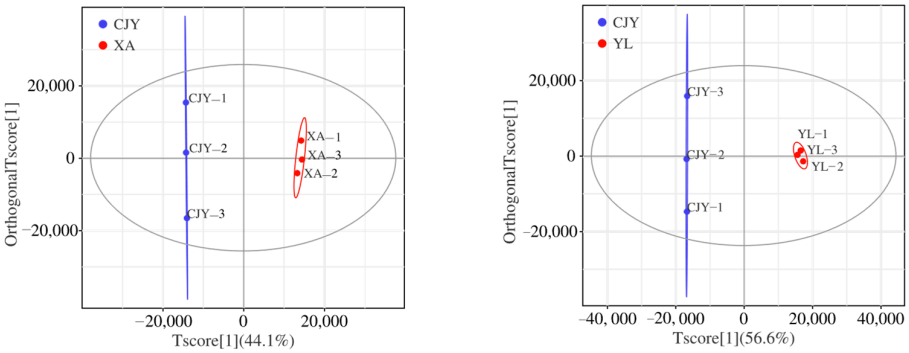


Figure 7. OPLS-DA score plots of three groups of metabolites.

Table 4. OPLS-DA model validation parameters.

Pair	R^2X (cum)	R^2Y (cum)	Q^2 (cum)
CJY-vs.-XA.POS	0.658	0.999	0.958
CJY-vs.-XA.NEG	0.695	0.996	0.923
CJY-vs.-YL.POS	0.698	1	0.988
CJY-vs.-YL.NEG	0.763	0.991	0.932

3.4.2. Identification and Analysis of Differential Metabolites

To visualize the significance of metabolite changes between samples, volcano plots and cluster heatmaps were plotted with VIP ≥ 1, $p < 0.05$, and FC ≥ 1. These are depicted in Figure 8. Figure 9 shows the top 20 metabolites in the VIP rankings for the two comparison groups: CJY vs. XA and CJY vs. YL. The screened differential metabolites were subjected

to KEGG pathway enrichment analysis, and Figure 10 shows the metabolic pathways that ranked in the top 18 of significance in both comparison groups.

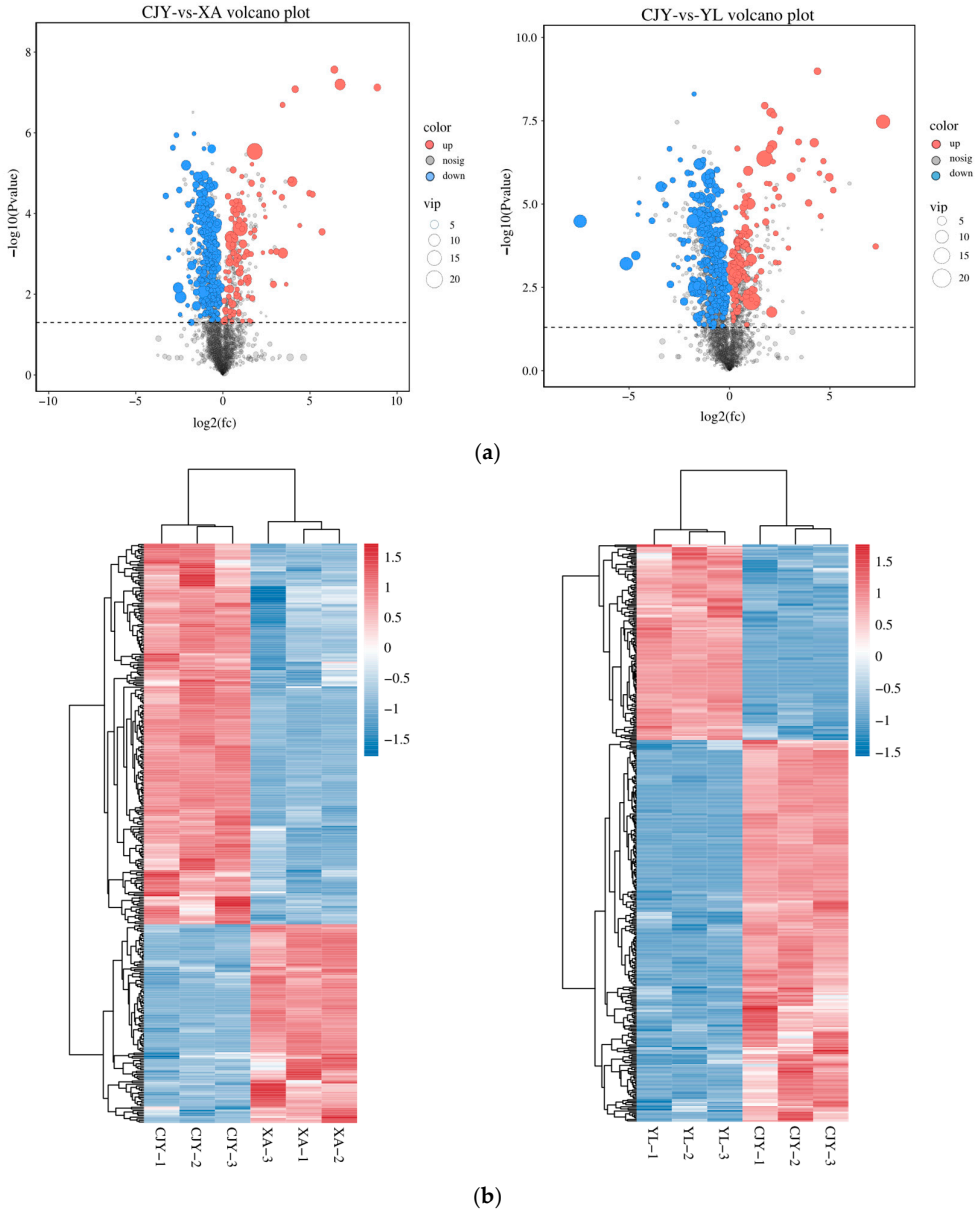


Figure 8. Visualization of VIP scores for differential metabolites. (**a**) Volcano plots of the metabolites CJY vs. XA and CJY vs. YL. (**b**) Cluster heatmaps of metabolites in two groups.

Under the screening criteria of VIP ≥ 1, $p < 0.05$, and FC ≥ 1, a total of 569 differential metabolites were screened between the XA and the CJY groups, with 261 metabolites up-regulated and 308 metabolites down-regulated. A total of 628 differential metabolites were screened between the YL and CJY groups, with 182 metabolites exhibiting up-regulation and 446 metabolites showing inhibition. The differential metabolites were classified into 12 primary categories, including lipid and lipid-like molecules, organic acids and derivatives, benzenes, and organoheterocyclic compounds. These significant metabolic changes indicated that the coal samples and their endogenous microbial communities significantly influenced the metabolic activities of the experimentally screened flora.

In the top 20 differential metabolites of VIP, seven differential metabolites were significantly up-regulated, and 13 differential metabolites were significantly down-regulated in the XA group compared to the CJY group. The up-regulated metabolites were mainly

carbohydrates and triterpenoids, such as D-gluconate and hecogenin. The down-regulated metabolites involved purine nucleosides, fatty acids, and steroids and steroid derivatives, such as adenosine, .gamma.-linolenic acid, and 17.alpha.-hydroxypregnenolone.

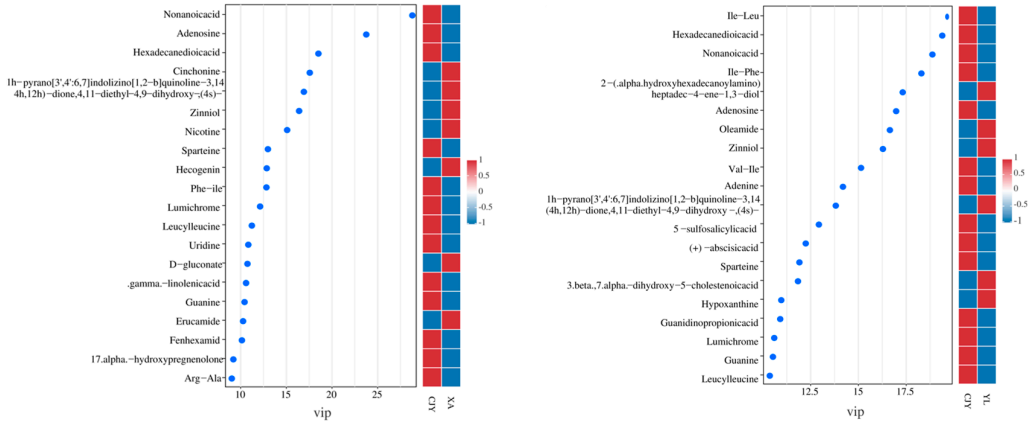


Figure 9. VIP plots of differential metabolites in the two groups.

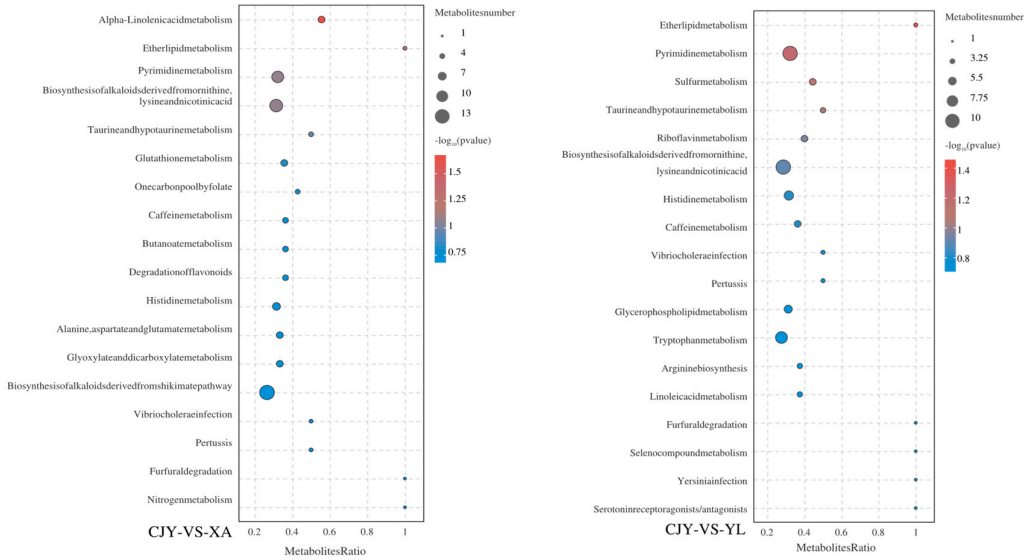


Figure 10. Enrichment analysis of KEGG pathway for differential metabolites.

In the YL group, six differential metabolites were significantly up-regulated, while 14 differential metabolites were significantly down-regulated compared with the CJY group. The up-regulated metabolites mainly included steroids and steroid derivatives and benzene and substituted derivatives, such as 3.beta.,7.alpha.-dihydroxy-5-cholestenoic acid and zinniol. Analyzing the reasons shows that there are molecular structures such as polycyclic aromatic hydrocarbons and aliphatic side chains in coal. The up-regulation of the aforementioned metabolites suggests that the microflora can destroy the macromolecular structures in YL coal samples to a certain extent, leading to the release of benzene ring derivatives and the generation of short-chain aliphatic compounds. The down-regulated metabolites were mainly amino acids, peptides and analogs, sesquiterpenoids, and purines and purine derivatives, such as Ile-Leu,(+)-abscisic acid and guanine.

In both comparison groups, the differential metabolites were significantly enriched in multiple metabolism-related signaling pathways, including lipid metabolism, nucleotide metabolism, amino acid metabolism, and energy metabolism, based on KEGG metabolic pathway enrichment analysis (Figure 10). It manifests in signaling pathways such as ether lipid metabolism, pyrimidine metabolism, taurine and hypotaurine metabolism, and the

biosynthesis of alkaloids derived from ornithine, lysine, and nicotinic acid, which are involved in a variety of aspects of membrane lipid synthesis, energy metabolism regulation, genetic material synthesis, and nutrient uptake in microorganisms. Furthermore, the differential metabolites between the CJY and XA groups were enriched in the nitrogen metabolism pathway; meanwhile, the sulfur metabolism pathway was significantly enriched in the YL group compared to the CJY group. These significant changes in metabolites as well as their participation in metabolic and signaling pathways reflected the adaptive regulation of microbial communities to externally added coal samples.

4. Discussion

During the growth phase, microbial communities exchange material and energy with the surrounding environment through a variety of catabolic and anabolic activities. Based on the results of the above analysis, it is clear that the addition of XA and YL coal samples has a significant effect on the metabolic activities of microbial communities, with the majority of the changes involving nitrogen and sulfur metabolism. Within 1 to 5 days of cultivation, the experimental system was dominated by metabolic pathways related to carbon metabolism, such as methane metabolism, glycolysis, and aliphatic metabolism, all of which are related to carbon metabolism. As the incubation time increased, the original substances in coal, such as sulfur-containing compounds and nitrogen-containing compounds, were widely utilized by the microbial communities. The degradation of original substances in coal, nutrient consumption in the cultivation system, and the generation of new substances all have a significant impact on microbial community growth. On the other hand, the utilization of nutrients by microbial communities accelerates the conversion of macromolecular molecules in coal into small molecular compounds. This improves targeted metabolic activities in microbial communities that can use newly generated compounds. The relative abundance of the carbon metabolism pathway was significantly reduced, while functional genes related to sulfur and nitrogen metabolism were significantly expressed, developing one of the cultivation system's major metabolic pathways and enhancing microbial energy metabolism activity. Combining the characteristics of the product changes in the gas and liquid phases of the experimental system with the results of metabolomics analysis, we explored the changes in key metabolic pathways of the microbial flora under the effect of different coal samples. These key metabolic pathways are depicted in Figure 11.

Microbial sulfur metabolism-related genes appeared to be differentially expressed to varying degrees under the effect of coal samples, regulating the metabolic levels of intracellular and extracellular sulfur-containing compounds accordingly. As can be seen in Figure 10, the sulfur metabolism pathways of the microbial community in the experimental system were mainly dominated by assimilatory sulfate and reduction, dissimilatory sulfate reduction and oxidation, as well as thiosulfate metabolism in the SOX system. Sulfate can be reduced to sulfite and sulfide by specific bacteria flora, a process that involves a variety of cellular life activities and produces many intermediate products such as APS (adenosine 5′-phosphosulfate) and [Dsrc protein]-trisulfide, while sulfide can be reoxidized to sulfite and sulfate under certain conditions to participate in the sulfur cycle. Sulfides are crucial endogenous signaling molecules that regulate a wide range of cellular activities [49]. Earlier research found that the final step in sulfate assimilation is Cys (cysteine) synthesis [50]. Cys is an intermediate carrier for microorganisms that converts inorganic sulfur elements into organic sulfur and participates in the metabolism of organisms, and its synthesis process is widely involved in cellular life activities, such as the metabolism of Gly, Ser, and Threonine (Thr), as well as methane metabolism.

Unlike sulfate, after entering the cell, thiosulfate can be catalyzed by 3-mercaptopyruvate sulfurtransferase or thiosulfate sulfurtransferasee to produce sulfite or oxidized to sulfate by

the SOX system [51]. In addition, it can be generated into sulfide under the catalytic action of cytochrome enzymes for Cys synthesis. It is worth noting that, in addition to sulfate, the culture environment may contain methyl thioether, which can be oxidized directly to dimethyl sulfoxide (DMSO) and dimethyl sulfone ($DMSO_2$) and finally converted to methane-sulfonate, sulfite, or sulfate. At the same time, methyl thioether can be converted to methyl-mercaptan and sulfide through certain functional enzymes, allowing it to participate in microbial sulfur metabolism.

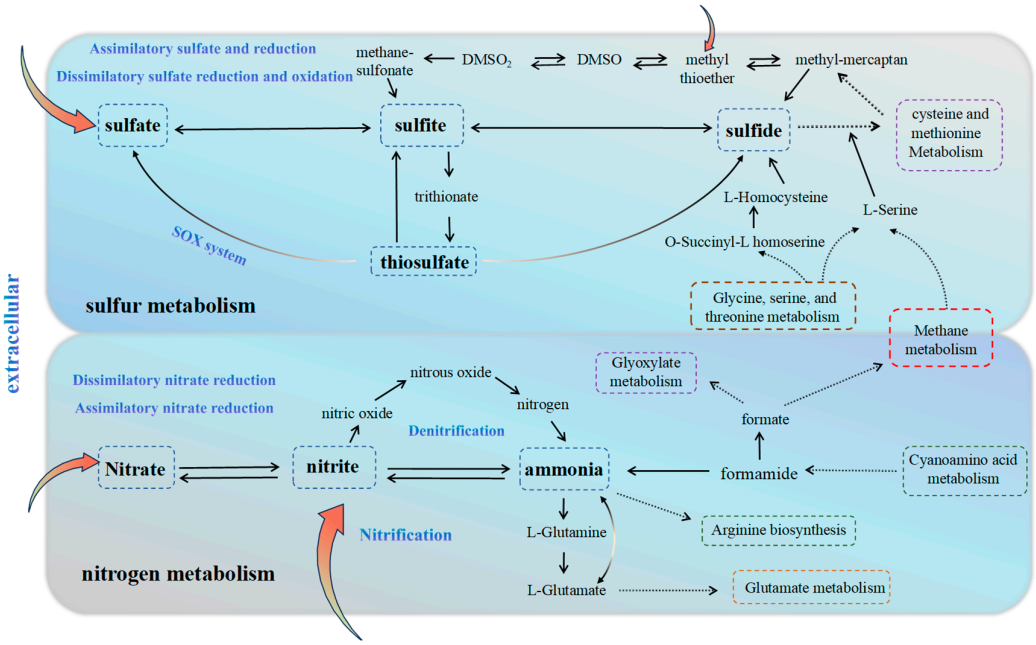


Figure 11. Microbial sulfur and nitrogen metabolism in the presence of different coal samples.

Following the addition of coal samples, both liquid-phase product analysis and metabolomics results from the experimental system showed significant changes in compounds containing nitrogen and nitrogen metabolic pathways. This shows that the experimental system has active nitrogen transformation potential in the presence of coal samples. Certain organic or inorganic components in coal may be released by degradation by specific bacteria, such as Pseudoxanthomonas [52] and Acidovorax [53], resulting in soluble nitrates and nitrites. These nitrates and nitrites can be transported to the cell's interior through Nrt transporter proteins, participating in the microbial nitrogen cycle [54]. Nitrate is reduced to nitrite by nitrate reductase (NR), and nitrite reductase (NiR) can convert nitrite to ammonia, which is then involved in nitrogen-containing compound metabolic pathways, such as glutamate (Glu) and arginine (Arg). Denitrification may also occur within the experimental system. Previous research has shown that Hyphomicrobium is often regarded as a key player in denitrification systems that use methanol as a carbon source [55]. The presence of Hyphomicrobium further indicates that denitrification occurs within the experimental system. During this process, nitrates and nitrites are gradually decreased and converted into gaseous nitrogen, which is eventually released into the culture environment. It should be noted that we analyzed potential nitrogen metabolism processes involving microorganisms in the experimental system based on metabolic function prediction and pathway enrichment. However, we do not include a systematic analysis of the specific concentrations of nitrogen-containing compounds, such as nitrate and nitrite, in the culture medium, or their interconversion relationships. There remain certain limitations in describing the dynamic changes in nitrogen metabolic products.

Currently, numerous research studies in various fields, such as environmental science and applied microbiology, have conducted quantitative analyses of nitrogen-containing transformation mechanisms in microbial environments. Ungwiwatkul et al. [56] utilized atmospheric plasma to promote nitrogen fixation. By quantitatively measuring the concentrations of nitrogen derivatives such as NO_2^-, NO_3^-, and NH_4^+, they revealed the primary pathways of nitrogen transformation in this process. Under the action of plasma, nitrogen and oxygen are excited to form NO and NO_2. These nitrogen oxides further react with water to form HNO_2 and HNO_3, which then dissociate into NO_2^- and NO_3^-. Simultaneously, free radical reactions promote the combination of nitrogen and hydrogen to form NH_3, which is subsequently protonated to yield NH_4^+. This study not only successfully explains the mechanism of nitrogen conversion from gaseous to soluble forms under plasma-driven conditions, but it also provides theoretical guidelines for future research. Similarly, nitrogen form monitoring results reported in studies show that dynamic changes in different nitrogen sources (e.g., ammonia nitrogen, nitrate, and nitrite) can accurately reflect the characteristics of microbial-dominated nitrogen metabolism processes [57,58]. These findings not only effectively explain the transformation processes of different forms of nitrogen during nitrogen metabolism but also provide support for the metabolic pathways discussed in this study. In contrast, this study focuses on the characteristics of microbial nitrogen metabolism changes through material functions and metabolic pathways, providing further understanding into nitrogen transformation mechanisms in complex environments.

5. Conclusions

(1) Coal-sourced flora accelerated O_2 consumption in the experimental systems, and the XA and YL groups ran out of O_2 on days 11 and 9, respectively. Within the first 9 days, the CH_4 consumption of the three groups was 63.84 mL, 57.64 mL, and 63.66 mL, respectively, indicating that the addition of XA and YL coal samples did not significantly inhibit the methane degradation efficiency of the methane-oxidizing communities. Instead, the addition of YL coal samples showed a strong promotion effect on the methane degradation ability of the flora under oxygen-enriched conditions.

(2) The addition of coal samples had a significant effect on the expression of sulfur and nitrogen metabolism pathways in the microbial community. The sulfur-containing components of coal were synergistically degraded and utilized by the microflora, resulting in a significant increase in SO_4^{2-} concentrations in the XA and YL groups compared to the CJY group. The concentration of NO_3^- in the three solutions increased and then decreased, with the YL group having the largest decrease in the latter stage, indicating a stronger ability to reduce nitrate.

(3) The amino acid metabolism of the microbial communities in the coal sample environment showed stage-specific characteristics. Initially, Pro and Cys were dominant. Glu and Asp levels increased significantly as the incubation period increased, indicating the enhancement of the microbial nitrogen metabolism function. At a later stage, the XA and YL groups were limited in their ability to oxidize methane due to O_2 depletion, which promoted the synthesis of Ser.

(4) Nutrient acquisition by the microbial communities drives coal degradation, and coal degradation products further stimulate these communities to enhance the metabolic pathways that target this. The addition of XA coal samples influenced the nitrogen pathway of the microbial communities, while YL coal samples significantly enhanced the sulfur metabolism pathway.

Author Contributions: Writing—original draft, H.M.; methodology, R.Z.; writing—review and editing, Y.Z.; investigation, K.T.; formal analysis, W.G.; validation, C.D. and S.C. All authors have read and agreed to the published version of the manuscript.

Funding: This work was supported by the National Natural Science Foundation of China (No. 52174168), the Program for Innovative Team and Talent in University of Henan (No. 22IRTSTHN009, No. 24HASTIT019), Key Research and Development Special Program of Henan Province (No. 241111320700), and Henan Provincial Association of Science and Technology Youth Talent Lift Project (NO. 2023HYTP014).

Data Availability Statement: The original contributions presented in this study are included in the article. Further inquiries can be directed to the corresponding author.

Conflicts of Interest: The authors declare that they have no known competing financial interests or personal relationships that could have appeared to influence the work reported in this paper.

Abbreviations

The following abbreviations are used in this manuscript:

PAH	Polycyclic Aromatic Hydrocarbons
EPS	Extracellular Polymeric Substances
M_{ad}	Moisture, air dried basis
A_d	Air-dry basis
V_{daf}	Volatile matter, dry ash-free basis
FC_{daf}	Fixed Carbon, dry ash-free basis
PCA	Principal Components Analysis
OPLS-DA	Orthogonal Partial Least Squares Discriminant Analysis
VIP	Variable Importance in Projection
FC	Fold Change
p	p-value
KEGG	Kyoto Encyclopedia of Genes and Genomes
DMSO	Dimethyl Sulfoxide
$DMSO_2$	Dimethyl Sulfone

References

1. Zhou, Y.; Zhang, R.; Tian, K.; Zhao, S.; Shi, H.; Gong, W.; Lei, Q. Characteristics of the Methanotroph Used in Coalbed Methane Emission Reduction: Methane Oxidation Efficiency and Coal Wettability. *Fuel* **2023**, *349*, 128596. [CrossRef]
2. Zhang, R.; Zhou, Y.; Yu, H.; Wang, S.; Ren, T. Experimental Investigation of the Use of Methanotrophs for the Degradation of Low-Concentration Methane. *Arab. J. Geosci.* **2021**, *14*, 685. [CrossRef]
3. Mimura, K.; Harada, M.; Sumiyoshi, S.; Toya, G.; Takagi, M.; Fujita, E.; Takata, A.; Tatetsu, S. Long-Term Effects of Carbon Monoxide Poisoning at Miike Coal Mine: A 33-Year Follow-up Study. *Undersea Hyperb. Med.* **2023**, *50*, 111–143. [CrossRef] [PubMed]
4. Xiong, H.; Ming, T.; Wu, Y.; Wang, C.; Chen, Q.; Li, W.; Mu, L.; de Richter, R.; Yuan, Y. Numerical Analysis of Solar Chimney Power Plant Integrated with CH4 Photocatalytic Reactors for Fighting Global Warming under Ambient Crosswind. *Renew. Energy* **2022**, *201*, 678–690. [CrossRef]
5. Cai, Y.; Zheng, Y.; Bodelier, P.L.E.; Conrad, R.; Jia, Z. Conventional Methanotrophs Are Responsible for Atmospheric Methane Oxidation in Paddy Soils. *Nat. Commun.* **2016**, *7*, 11728. [CrossRef]
6. Joon, U.K.; Sun, M.K.; Yun, K.K.; Yun, H.J. A Study on Optimum Ventilation System in the Deep Coal Mine. *ResearchGate* **2025**, *25*, 186–198.
7. Zhang, C.; Li, Y. Optimization of Directional Long Boreholes Unloading Gas Extraction Process and Application Research. *Appl. Sci.* **2025**, *15*, 230. [CrossRef]
8. Lou, Z.; Wang, K.; Kang, M.; Zhao, W.; Wei, G.; Yue, J.; Yao, H. Plugging Methods for Underground Gas Extraction Boreholes in Coal Seams: A Review of Processes, Challenges and Strategies. *Gas Sci. Eng.* **2024**, *122*, 205225. [CrossRef]
9. Zhang, Z.; Wang, H.; Deng, B.; Li, M.; Zhang, D. Field Investigation of Hydraulic Fracturing in Coal Seams and Its Enhancement for Methane Extraction in the Southeast Sichuan Basin, China. *Energies* **2018**, *11*, 3451. [CrossRef]
10. Limbri, H.; Gunawan, C.; Thomas, T.; Smith, A.; Scott, J.; Rosche, B. Coal-Packed Methane Biofilter for Mitigation of Green House Gas Emissions from Coal Mine Ventilation Air. *PLoS ONE* **2014**, *9*, e94641. [CrossRef]
11. Han, Y.; Xu, L.; Zhang, R.; Lv, J.; Yang, F.; Ma, C. Study on Methane Degradation by Microbial Agents Based on Chelating Wetting Agent Carriers. *Sci. Rep.* **2024**, *14*, 15420. [CrossRef] [PubMed]

12. Xie, J.; Sun, X.; Du, H.; Chen, D.; Wang, Y. Exploring the Effects of Different Methane and Oxygen Concentrations on the Methane-Oxidizing Bacteria Mixed Community. *J. Environ. Eng.* **2023**, *149*, 04023081. [CrossRef]
13. Liu, D.; Yang, Y.; Ai, J.; Li, Y.; Xing, Y.; Li, J. Research on Microbial Structures, Functions and Metabolic Pathways in an Advanced Denitrification System Coupled with Aerobic Methane Oxidation Based on Metagenomics. *Bioresour. Technol.* **2021**, *332*, 125047. [CrossRef]
14. Jung, G.; Rhee, S.; Han, Y.; Kim, S. Genomic and Physiological Properties of a Facultative Methane-Oxidizing Bacterial Strain of Methylocystis Sp. from a Wetland. *Microorganisms* **2020**, *8*, 1719. [CrossRef] [PubMed]
15. Xu, S.; Zhang, H. First Evidence for Anaerobic Oxidation of Methane Process in Landfill Cover Soils: Activity and Responsible Microorganisms. *Sci. Total Environ.* **2022**, *841*, 156790. [CrossRef]
16. Asakawa, S. Ecology of Methanogenic and Methane-Oxidizing Microorganisms in Paddy Soil Ecosystem. *Soil Sci. Plant Nutr.* **2021**, *67*, 520–526. [CrossRef]
17. Paul, B.G.; Ding, H.; Bagby, S.C.; Kellermann, M.Y.; Redmond, M.C.; Andersen, G.L.; Valentine, D.L. Methane-Oxidizing Bacteria Shunt Carbon to Microbial Mats at a Marine Hydrocarbon Seep. *Front. Microbiol.* **2017**, *8*, 186. [CrossRef]
18. Yu, Z.; Chistoserdova, L. Communal Metabolism of Methane and the Rare Earth Element Switch. *J. Bacteriol.* **2017**, *199*, e00328-17. [CrossRef]
19. Jiang, L.; Chu, Y.; Zhang, X.; Wang, J.; He, X.; Liu, C.; Chen, T.; He, R. Characterization of Anaerobic Oxidation of Methane and Microbial Community in Landfills with Aeration. *Environ. Res.* **2022**, *214*, 114102. [CrossRef]
20. Xu, K.; Yan, Z.; Tao, C.; Wang, F.; Zheng, X.; Ma, Y.; Sun, Y.; Zheng, Y.; Jia, Z. A Novel Bioprospecting Strategy via 13C-Based High-Throughput Probing of Active Methylotrophs Inhabiting Oil Reservoir Surface Soil. *Sci. Total Environ.* **2024**, *924*, 171686. [CrossRef]
21. Ding, J.; Lu, Y.; Fu, L.; Ding, Z.; Mu, Y.; Cheng, S.H.; Zeng, R.J. Decoupling of DAMO Archaea from DAMO Bacteria in a Methane Driven Microbial Fuel Cell. *Water Res.* **2017**, *110*, 112–119. [CrossRef] [PubMed]
22. Jiang, H.; Duan, C.; Luo, M.; Xing, X. Enrichment and Characteristics of Mixed Methane-Oxidizing Bacteria from a Chinese Coal Mine. *Appl. Microbiol. Biotechnol.* **2016**, *100*, 10331–10341. [CrossRef] [PubMed]
23. Pytlak, A.; Sparkes, R.; Goraj, W.; Szafranek-Nakonieczna, A.; Banach, A.; Akhmetkaliyeva, S.; Slowakiewicz, M. Methanotroph-Derived Bacteriohopanepolyol Signatures in Sediments Covering Miocene Brown Coal Deposits. *Int. J. Coal Geol.* **2021**, *242*, 103759. [CrossRef]
24. Xie, J.; Yang, Q.; Wang, Y.; Chen, D.; Zhang, J.; Yue, Z.; Lyu, J. Research on Coal Mine Gas Microbial Degradation Device Based on Charcoal Filling Material. *ACS Omega* **2025**, *10*, 28932–28943. [CrossRef]
25. Zhou, Y.; Zhang, R.; Tian, K.; Ma, H.; Zhao, S.; Gong, W.; Duan, C.; Chu, S. Adsorption Characteristics of Methanotrophic Bacteria in Coalbed Methane Emission Reduction. *Chem. Eng. J.* **2025**, *519*, 164825. [CrossRef]
26. Dong, Y.; Liu, Y.; Lin, H.; Liu, C. Improving Vanadium Extraction from Stone Coal via Combination of Blank Roasting and Bioleaching by ARTP-Mutated Bacillus Mucilaginosus. *Trans. Nonferrous Met. Soc. China* **2019**, *29*, 849–858. [CrossRef]
27. Li, Q.; Dong, F.; Dai, Q.; Zhang, C.; Yu, L. Surface Properties of PM2.5 Calcite Fine Particulate Matter in the Presence of Same Size Bacterial Cells and Exocellular Polymeric Substances (EPS) of Bacillus Mucitaginosus. *Environ. Sci. Pollut. Res.* **2018**, *25*, 22429–22436. [CrossRef]
28. Gataraddi, S.; Aladakatti, R.H.; Patil, S.J.; Sadashiv, S.O. Microbe–Mineral Interactions: Environmental Pollution and Management. In *Biotechnology for Environmental Sustainability*; Springer: Singapore, 2025.
29. David, Y.; Baylon, M.G.; Pamidimarri, S.D.V.N.; Baritugo, K.-A.; Chae, C.G.; Kim, Y.J.; Kim, T.W.; Kim, M.-S.; Na, J.G.; Park, S.J. Screening of Microorganisms Able to Degrade Low-Rank Coal in Aerobic Conditions: Potential Coal Biosolubilization Mediators from Coal to Biochemicals. *Biotechnol. Bioprocess Eng.* **2017**, *22*, 178–185. [CrossRef]
30. Ma, S.; Zong, Q. Exploration and Application of Microbial Method to Enhance the Effect of Hydraulic Fracturing on Coal Seam Permeability Enhancement and Gas Extraction. *Energy Explor. Exploit.* **2024**, *42*, 837–855. [CrossRef]
31. Liu, C.; Ma, S.; Wang, X.; Ou, Y.; Du, H. Biodegradation of Organic Compounds in the Coal Gangue by Bacillus Sp. into Humic Acid. *Biodegradation* **2023**, *34*, 125–138. [CrossRef]
32. Xu, Z.; Zhang, L.; Gao, Y.; Tan, X.; Sun, Y.; Chen, W. Effects of Coal Mining Activities on the Changes in Microbial Community and Geochemical Characteristics in Different Functional Zones of a Deep Underground Coal Mine. *Water* **2024**, *16*, 1836. [CrossRef]
33. Zhu, Q.; Ruan, M.; Hu, Z.; Miao, K.; Ye, C. The Relationship between Acid Production and the Microbial Community of Newly Produced Coal Gangue in the Early Oxidation Stage. *Microorganisms* **2023**, *11*, 2626. [CrossRef] [PubMed]
34. Zhang, W.; Mo, Q.; Huang, Z.; Sabar, M.A.; Medunic, G.; Ivosevic, T.; He, H.; Urynowicz, M.; Liu, F.-J.; Guo, H.; et al. Contaminants from a Former Croatian Coal Sludge Dictate the Structure of Microbiota in the Estuarine (Rasa Bay) Sediment and Soil. *Front. Microbiol.* **2023**, *14*, 1126612.
35. Lian, Z.; Yang, Z.; Song, W.; Sun, M.; Gan, Y.; Bai, X. Characteristics of EPS from Pseudomonas Aeruginosa and Alcaligenes Faecalis under Cd(II) Stress: Changes in Chemical Components and Adsorption Performance. *Environ. Sci. Pollut. Res.* **2022**, *29*, 75883–75895. [CrossRef] [PubMed]

36. Jones, D.L.; Edwards, A.C. Influence of Sorption on the Biological Utilization of Two Simple Carbon Substrates. *Soil Biol. Biochem.* **1998**, *30*, 1895–1902. [CrossRef]
37. DIAB, S.; Shilo, M. Effect of Adhesion to Particles on the Survival and Activity of *Nitrosomonas* sp. and *Nitrobacter* sp. *Arch. Microbiol.* **1988**, *150*, 387–393.
38. Keen, G.A.; Prosser, J.I. The Surface Growth and Activity of Nitrobacter. *Microb. Ecol.* **1988**, *15*, 21–39. [CrossRef]
39. Zhang, Y.; Wang, N.; Zhang, B.; Zhang, W.; Shen, B. Interannual Variation and Chemical Characterization of Major Water-Soluble Inorganic Ions in Snow across Northwest China. *Front. Earth Sci.* **2023**, *11*, 1099178. [CrossRef]
40. Reis, P.C.J.; Tsuji, J.M.; Weiblen, C.; Schiff, S.L.; Scott, M.; Stein, L.Y.; Neufeld, J.D. Enigmatic Persistence of Aerobic Methanotrophs in Oxygen-Limiting Freshwater Habitats. *ISME J.* **2024**, *18*, wrae041. [CrossRef]
41. Rout, P.G.; Mohanty, A.K.; Pradhan, N.; Biswal, S.K.; Behera, S.K. Study on the Reaction Mechanism of Oxidative Microbial Desulfurization of Organic Sulfur-Rich Coal. *Geomicrobiol. J.* **2022**, *39*, 210–218. [CrossRef]
42. Ai, C.; Xue, S.; Liu, C.; Wang, S. Optimization of Experimental Conditions and Study of Desulfurization Mechanism of *Rhodococcus erythropolis* for Organic Sulfur Removal from Coal. *J. Environ. Chem. Eng.* **2025**, *13*, 116103. [CrossRef]
43. Gotz, F.; Longnecker, K.; Soule, M.C.K.; Becker, K.W.; McNichol, J.; Kujawinski, E.B.; Sievert, S.M. Targeted Metabolomics Reveals Proline as a Major Osmolyte in the Chemolithoautotroph Sulfurimonas Denitrificans. *MicrobiologyOpen* **2018**, *7*, e586. [CrossRef] [PubMed]
44. Wang, L.; Guo, Y.; Shen, Y.; Yang, K.; Cai, X.; Zhang, B.; Liu, Z.; Zheng, Y. Microbial Production of Sulfur-Containing Amino Acids Using Metabolically Engineered *Escherichia coli*. *Biotechnol. Adv.* **2024**, *73*, 108353. [CrossRef] [PubMed]
45. Li, R.; Wang, J.; Yuan, H.; Niu, Y.; Sun, J.; Tian, Q.; Wu, Y.; Yu, J.; Tang, Z.; Xiao, X.; et al. Exogenous Application of ALA Enhanced Sugar, Acid and Aroma Qualities in Tomato Fruit. *Front. Plant Sci.* **2023**, *14*, 1323048. [CrossRef]
46. McDonald, I.R.; Murrell, J.C. The Methanol Dehydrogenase Structural Gene mxaF and Its Use as a Functional Gene Probe for Methanotrophs and Methylotrophs. *Appl. Environ. Microbiol.* **1997**, *63*, 3218–3224. [CrossRef]
47. Crowther, G.J.; Kosaly, G.; Lidstrom, M.E. Formate as the Main Branch Point for Methylotrophic Metabolism in Methylobacterium Extorquens AM1. *J. Bacteriol.* **2008**, *190*, 5057–5062. [CrossRef]
48. Wang, Y.; Fan, L.; Tuyishirne, P.; Zheng, P.; Sun, J. Synthetic Methylotrophy: A Practical Solution for Methanol-Based Biomanufacturing. *Trends Biotechnol.* **2020**, *38*, 650–666. [CrossRef]
49. Aroca, A.; Benito, J.M.; Gotor, C.; Romero, L.C. Persulfidation Proteome Reveals the Regulation of Protein Function by Hydrogen Sulfide in Diverse Biological Processes in Arabidopsis. *J. Exp. Bot.* **2017**, *68*, 4915–4927. [CrossRef]
50. Kawano, Y.; Onishi, F.; Shiroyama, M.; Miura, M.; Tanaka, N.; Oshiro, S.; Nonaka, G.; Nakanishi, T.; Ohtsu, I. Improved Fermentative L-Cysteine Overproduction by Enhancing a Newly Identified Thiosulfate Assimilation Pathway in *Escherichia coli*. *Appl. Microbiol. Biotechnol.* **2017**, *101*, 6879–6889. [CrossRef]
51. Feng, S.; Yang, H.; Wang, W. System-Level Understanding of the Potential Acid-Tolerance Components of Acidithiobacillus Thiooxidans ZJJN-3 under Extreme Acid Stress. *Extremophiles* **2015**, *19*, 1029–1039. [CrossRef]
52. Luan, Y.; Xu, Y.; Guo, Z.; Yin, Y.; Wang, Q.; Zhang, F.; Xiao, Y.; Liu, C.; Jiang, S. Enhanced Nitrogen Removal in Immersed Rotating Self-Aerated Biofilm Reactor: Nitrogen Removal Pathway and Microbial Mechanism. *Bioresour. Technol.* **2023**, *385*, 129426. [CrossRef]
53. Blohm, A.; Kumar, S.; Knebl, A.; Herrmann, M.; Kuesel, K.; Popp, J.; Frosch, T. Activity and Electron Donor Preference of Two Denitrifying Bacterial Strains Identified by Raman Gas Spectroscopy. *Anal. Bioanal. Chem.* **2022**, *414*, 601–611. [CrossRef] [PubMed]
54. Li, B.; Wang, X.; Li, Q.; Xu, D.; Li, J.; Hou, W.-T.; Chen, Y.; Jiang, Y.-L.; Zhou, C.-Z. Allosteric Regulation of Nitrate Transporter NRT via the Signaling Protein PII. *Proc. Natl. Acad. Sci. USA* **2024**, *121*, e2318320121. [CrossRef] [PubMed]
55. Martineau, C.; Mauffrey, F.; Villemur, R. Comparative Analysis of Denitrifying Activities of Hyphomicrobium Nitrativorans, Hyphomicrobium Denitrificans, and Hyphomicrobium Zavarzinii. *Appl. Environ. Microbiol.* **2015**, *81*, 5003–5014. [CrossRef]
56. Ungwiwatkul, S.; Jaikua, M.; Prasertboonyai, K.; Thana, P.; Tamman, A.; Matra, K. Plasma-Activated Municipal Wastewater (PAMW): Revolutionizing Municipal Wastewater into High-Value Liquid Fertilizer for Duckweed Cultivation through Air Plasma Treatment. *Appl. Sci. Eng. Prog.* **2025**, *18*, 7791. [CrossRef]
57. Xuan, Y.; Mai, Y.; Xu, Y.; Zheng, J.; He, Z.; Shu, L.; Cao, Y. Enhanced Microbial Nitrification-Denitrification Processes in a Subtropical Metropolitan River Network. *Water Res.* **2022**, *222*, 118857. [CrossRef]
58. Ouyang, L.; Thamdrup, B.; Trimmer, M. Coupled Nitrification and N2 Gas Production as a Cryptic Process in Oxic Riverbeds. *Nat. Commun.* **2021**, *12*, 1217. [CrossRef]

Disclaimer/Publisher's Note: The statements, opinions and data contained in all publications are solely those of the individual author(s) and contributor(s) and not of MDPI and/or the editor(s). MDPI and/or the editor(s) disclaim responsibility for any injury to people or property resulting from any ideas, methods, instructions or products referred to in the content.